An Experimental Study on Stripe Pattern Formation of Ag−Sb Electrodeposits

M. Saitou* and Y. Fukuoka

Department of Mechanical Systems Engineering, University of the Ryukyus, 1 Senbaru Nishihara-cho, Okinawa, Japan, 903-0213

Received: November 14, 2003; In Final Form: February 23, 2004

Transient changes in surface morphologies of Ag−Sb thin films electrodeposited from an aqueous electrolyte have been studied. Measurements of the potential and current density applied during electrodeposition reveal that stripe patterns that comprise bright and dark regions are formed within a small range of the potential and current density that exhibits no oscillatory behavior. In addition, the experimental results on the transient current density are found to be in good agreement with the solutions of unsteady diffusion equations, whose results give the ratios of the kinetic constants to the diffusion coefficient that may be related to a necessary condition for the Turing instability in reaction−diffusion systems. Fourier analysis of the time-series stripe images shows that stripe spacings change with the area ratio of the bright regions to the dark regions fixed. This indicates that the stripe patterns formed at the different deposition times emerge on different length-scales.

Introduction

Spatial pattern formation that emerges in nonequilibrium and irreversible systems, which abound in nature, has been actively studied in physical, chemical, and biological fields.[1−2] One aim of these research studies is to clarify the origin of pattern formation that allows us to describe them with a few factors related to universality classes. Turing pattern that has been investigated both experimentally[3] and theoretically,[4] is a good candidate for the mechanisms of pattern formation due to the diffusion-driven instability. Linear instability analysis applies to the Turing instability in reaction−diffusion systems and leads a necessary condition for the Turing instability, which is often referred to as local activation and long-range inhibition.[5]

Pattern formation in single-element electrodeposition that appears in various morphologies has been early recognized, which has a physical feature that is well captured by diffusion-limited aggregates (DLA).[6] Recent progress in surface morphologies of thin films electrodeposited from aqueous electrolytes reveals that surface roughening obeys simple scaling relations characterized by scaling exponents.[7] Characteristic patterns in Ag−In[8] and Ag−Sb[9,10] electrodeposits as well as spiral patterns in the famous chlorite−iodide−malonic acid (CIMA)[3] and Belousov-Zhabotinsky (BZ)[5] reactions were reported but no quantitative investigations into the transient surface morphologies were carried out.

In this paper, we present new experimental results on stripe patterns of Ag−Sb thin films electrodeposited on copper substrates. First, a potential impulse[11,12] represented by a step function applies across electrochemical circuits, and current density−time curves passing through the electrochemical cell during electrodeposition are recorded. Experimental conditions under which the stripe patterns emerge are examined with the electric measurements and microscope images of the Ag−Sb thin films. Fitting an analytical solution for a kinetic electrocrystallization model of Ag and Sb ions to the measured current density−time curves, we determine the ratios of the kinetic constants and diffusion coefficients for Ag and Sb ions, which are discussed in views of the Turing instability condition in reaction−diffusion systems. Second, to clarify periodic properties of the time-series stripe patterns, the Fourier transformation is used in the digitized images observed with a laser profile microscope. This surface morphology observation will lead one to the conclusion that the stripe patterns are represented by average stripe spacings and have a time-invariant property.

Experiment

Experiments were performed using an electrolyte that includes the following components (g/L): $AgNO_3$ 25.5; $K_4Fe(CN)_6 \cdot 3H_2O$, 72; KSCN, 146; $KNaC_4H_4O_6 \cdot 4H_2O$, 59.3; $C_8H_4K_2O_{12}Sb_2 \cdot 3H_2O$ (APT), 6.7, 10, 13.3, and 20.1; K_2CO_3, 31.3. The mixed solution of $AgNO_3$, K_2CO_3, and $K_4Fe(CN)_6 \cdot 3H_2O$, which was boiled for 30 min and prepared for silver cyanide complexes, yielded burnt umber precipitates of iron hydroxides. After removal of the iron hydroxide, the remaining components were added into the solution.

Poly-crystalline copper and carbon plates 20 mm long and 10 mm wide were prepared for working and counter electrodes, respectively. The copper substrates of 99.9 wt % purity appear to be mirrorlike. These electrodes cleaned by a wet process were located parallel in a still cell including the chemical compositions mentioned above. A potential impulse was applied across the electrochemical cell and resistor as shown in Figure 1. The current through the electric cell was calculated from the potential drop across the resistor. We define the current density as the current through the electrochemical cell per unit cathode electrode area. Transient current (potential)−time curves passing through the cell maintained at 300 K during electrodeposition were recorded using the electric circuit and digital oscilloscope. Several resistors R ranging from 40 to 100 Ω were chosen to change current−potential characteristics of the cell. Ag−Sb deposits were grown on the copper substrates for the deposition time from 60 to 600 s.

* Corresponding author. Tel: +81-98-895-8635. Fax: 81-98-895-8707. E-mail: saitou@tec.u-ryukyu.ac.jp.

10.1021/jp0374760 CCC: $27.50
Published on Web 04/02/2004

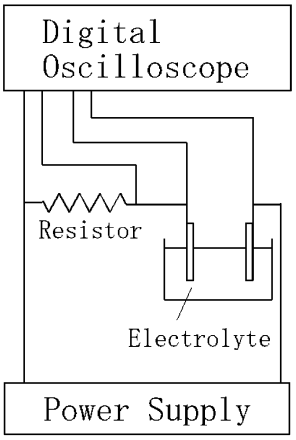

Figure 1. Schematic diagram of a simple electric circuit for measurements of transient current densities passing through the electrochemical cell and resistor R. Fixed potential impulses E_o are applied across the electrochemical cell and the resistor.

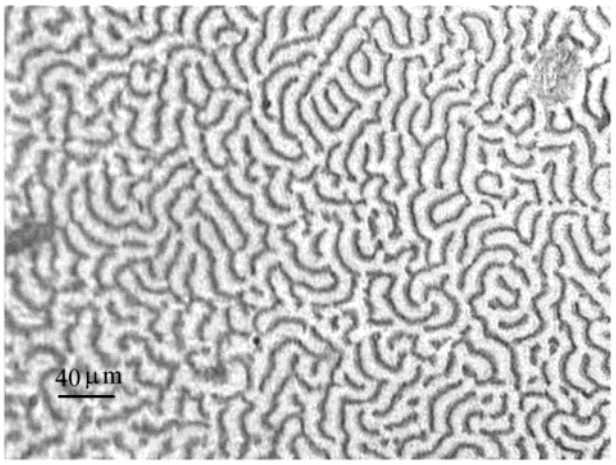

Figure 2. A typical microscope image of the Ag−Sb electrodeposit grown from the electrolyte of APT 6.7 g/L at $E_o = 2.20$ V, $R = 50\ \Omega$ and a growth time of 300 s.

The surface morphologies were observed with a laser profile microscope with accuracy of the order of 0.23 μm and were analyzed using the digitized microscope surface images with a resolution of 780 × 564 pixels. The Sb concentration in the Ag−Sb electrodeposits was determined by Electron Probe Micro-Analyzer (EPMA).

Results and Discussion

A typical microscope image from the sample electrodeposited at 300 s from the electrolyte including 6.7 g/L APT is shown in Figure 2. The surface image seems to be stripe patterns that are comprised of bright and dark regions. The dark regions have been reported to correspond to Sb-rich Ag electrodeposits.[9] The observed pattern is very similar to the patterns produced by computer simulations[2,13] based on the reaction−diffusion systems. In general, the reaction−diffusion systems have the drawback that quantitative comparisons with experiments remain difficult owing to many chemical reactions that include undetected intermediates. However, they give us some important insights into interpretations of experimental results.

Linear instability analysis[1,5] of the reaction−diffusion systems leads to conclusions that (1) pattern formation in chemical systems including at least two interacting chemicals occurs if their diffusion coefficients differ, and (2) diffusion destabilizes chemical systems at a particular wavelength. For activator−inhibitor systems including two reaction species, a necessary condition for the Turing instability[5] that is referred to as local activation and lateral inhibition is derived,

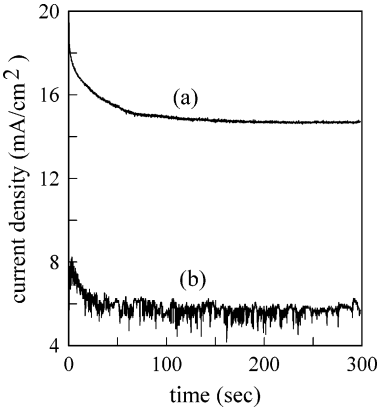

Figure 3. A plot of the current density vs the deposition time for two different APT concentrations in the electrolyte at $E_o = 2.4$ V and $R = 75\ \Omega$. (a) 6.7 g/L, (b) 20.1 g/L.

$$D_2/D_1 > |k_{22}/k_{11}| \tag{1}$$

where D_1 and D_2 are the diffusion coefficients of the activator and the inhibitor, and k_{11} and k_{22} are the reaction rates for the activator and the inhibitor, respectively. This indicates that the diffusion coefficients D_1 and D_2 should not have anisotropic values but different values that exceed the ratio $|k_{22}/k_{11}|$. To gain insights into experimental conditions for pattern formation in Ag−Sb electrodeposition, we determine the ratios of the kinetic constants to the diffusion coefficients of Ag and Sb ions. These quantities can be obtained from measurements of transient current density−time curves passing through electrochemical cells, and from analytical solutions of electrode reactions near cathode electrodes.

1. Transient Current−Time Curves. Two kinds of transient current densities passing through the cell were observed using the electric circuit in Figure 1. When the stripe patterns emerge, the current density recorded by the digital oscilloscope is stable (Figure 3 (a)), which phenomenon is independent of the APT concentration. As opposed to Figure 3(a), when the current density shows unstable or oscillatory behaviors (Figure 3(b)), no stripe pattern is observed. These strong fluctuations of the current density seem to be related to the rough surface morphology of the deposits. The electrodeposit surfaces do not appear to be mirrorlike whereupon the oscillations or unstable behaviors of the current density can be seen.

From the figure, we can see that both current densities decrease in the initial stage and plateau in the late stage, which current is defined as a saturated current density. In a similar way, the transient potential over the electrochemical cell plateaus, which is defined as a saturated potential. This means that electric resistance in the cell increases as a result of the development of a diffusion layer near the cathode electrode.

We consider the stripe pattern formation to be related to electrochemical processes in electrolyte for the following reasons: (a) the adions that reach the electrode are not affected by the electrical field normal to the electrode surface (see Figure 6, the potential affects the stripe pattern formation). The surface diffusion of the adions is not related to the stripe formation; (b) after the current flows between the anode and cathode electrode, it takes some time to produce the stripe pattern on the Ag−Sb electrodeposits (see Figure 7(a)), which suggests that some electrochemical species are needed to form the stripe

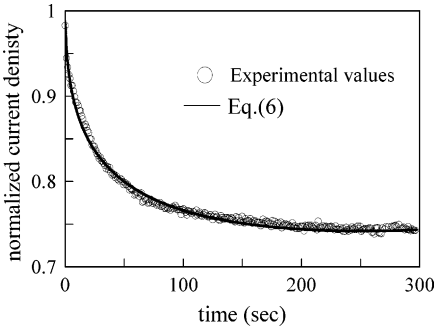

Figure 4. A plot of the normalized current density as a function of the deposition time. The solid line represents the calculated values for $k_1/\sqrt{D_1} = 0.2182$, $k_2/\sqrt{D_2} = 4.30 \times 10^{-2}$ s$^{-1/2}$ and $k_3' = 3.965 \times 10^{-5}$ mol/s. The circles indicate the experimental values measured for 13.3 g/L APT in the electrolyte at $E_o = 2.5$ V and $R = 75\ \Omega$.

patterns; (c) Figure 7, which shows variation of the stripe spacing with time, indicates that a white (dark) stripe does not always continue to grow on a white (dark) stripe, i.e., electrodeposition proceeds despite the electrodeposit surfaces. This suggests that the stripe pattern formation is related to the electrochemical process.

The electrochemical reactions in Ag−Sb electrodeposition are considered to proceed according to the following eq 2, which is often presented in the literature,[14−15]

$$[Ag(CN)_2(CNS)_m]^{-(m+1)} + e^- \xrightarrow{k_1} Ag + 2CN^- + mCNS^-$$

$$SbO^+ + 2H^+ + 3e^- \xrightarrow{k_2} Sb + H_2O$$

$$2CN^- + mCNS^- + Ag^+ \xrightarrow{k_3} [Ag(CN)_2(CNS)_m]^{-(m+1)} \quad (2)$$

where k_i is the rate constant and m has a value ranging from 1 to 2. APT is known to release SbO^+; moreover, CN and SCN ions are extensively known to play a role of complex agents that change the deposition potential. The third reaction in eq 2 represents formation of the Ag complexing agent due to a little decrease in $Ag(CN)_2(CNS)_m$ in the diffusion layer.

The change of the Ag complexing agent at the distance x and $x + dx$ from the cathode electrode at $x = 0$ due to the third reaction in eq 2 is given by $\partial C_1/\partial t = k_3[Ag^+]^2[CN^-]^2[CNS^-]^m$, where C_1 is the concentration of Ag complexing agent. As the concentrations of Ag^+, CN^-, and CNS^- are sufficiently high, the change can be approximated as $\partial C_1/\partial t = k_3'$ where k_3' is constant. Hence, the total changes in the concentrations and boundary conditions in one dimension are given by

$$\frac{\partial C_1}{\partial t} = D_1\frac{\partial^2 C_1}{\partial x^2} + k_3' \quad (3)$$

$$\frac{\partial C_2}{\partial t} = D_2\frac{\partial^2 C_2}{\partial x^2} \quad (4)$$

$$D_i\frac{\partial C_i}{\partial x} = k_i C_i, \text{ at } x = 0 \text{ and } i = 1,2 \quad (5)$$

$$C_i(x,0) = C_i^\circ,\ C_i(\infty,t) = C_i^\circ,\ i=1,2 \quad (6)$$

where C_2 is the concentration of SbO^+ ions, D_i is the diffusion coefficient, and C_i° is the equilibrium concentration. The

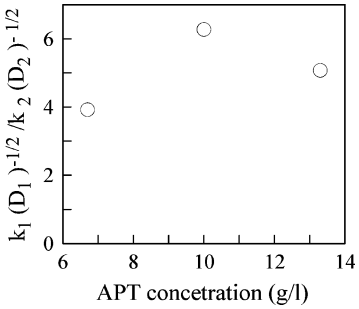

Figure 5. A plot of the ratio of $k_1(D_1)^{-1/2}/k_2(D_2)^{-1/2}$ best fitted to the measured current density−time curves for three different APT concentrations in the electrolyte.

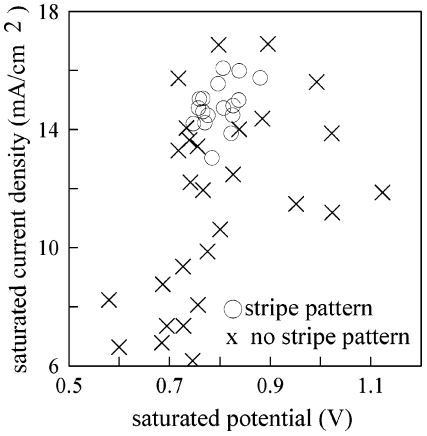

Figure 6. The saturated potential and current density phase diagram that represents the domain in which the stripe patterns are formed. The circles indicate that the stripe pattern is formed and the x symbols indicate that no stripe pattern is formed.

current density i is given by the number of flux converted to amperes,

$$i = \sum_{j=1}^{2} n_j F D_j \frac{\partial C_j}{\partial x}|_{x=0} \quad (7)$$

where n_j is the number of electrons transferred per ion, and F is Faraday's constant. Substitution of the solution C_i into eq 7, which is easily solved by the method of the Laplace transformation from tables,[16] leads to

$$i_1 = n_1 F k_1 \left[C_1^\circ e^{(k_1/\sqrt{D_1})^2 t}\mathrm{erfc}\left(\frac{k_1}{\sqrt{D_1}}\sqrt{t}\right) + k_3' \int_0^t e^{(k_1\sqrt{/D_1})^2\theta}\mathrm{erfc}\left(\frac{k_1}{\sqrt{D1}}\sqrt{\theta}\right) d\theta \right] \quad (8)$$

$$i_2 = n_2 F k_2 C_2^\circ e^{(k_2/\sqrt{D_2})^2 t}\mathrm{erfc}\left(\frac{k_2}{\sqrt{D_2}}\sqrt{t}\right) \quad (9)$$

$$\frac{i}{i_o} = \frac{F}{i_o}\sum_{j=1}^{2} n_j k_j C_j^\circ e^{(k_j/\sqrt{/D_j})^2 t}\mathrm{erfc}\left(\frac{k_j}{\sqrt{D_j}}\sqrt{t}\right) + \frac{n_1 F k_1 k_3'}{i_o}\int_0^t e^{(k_1/\sqrt{/D_1})^2\theta}\,\mathrm{erfc}\left(\frac{k_1}{\sqrt{D_1}}\sqrt{\theta}\right) d\theta \quad (10)$$

where $i_o = \Sigma_{i=1}^2 n_i F k_i C_i^\circ$, and erfc is the complementary error function.

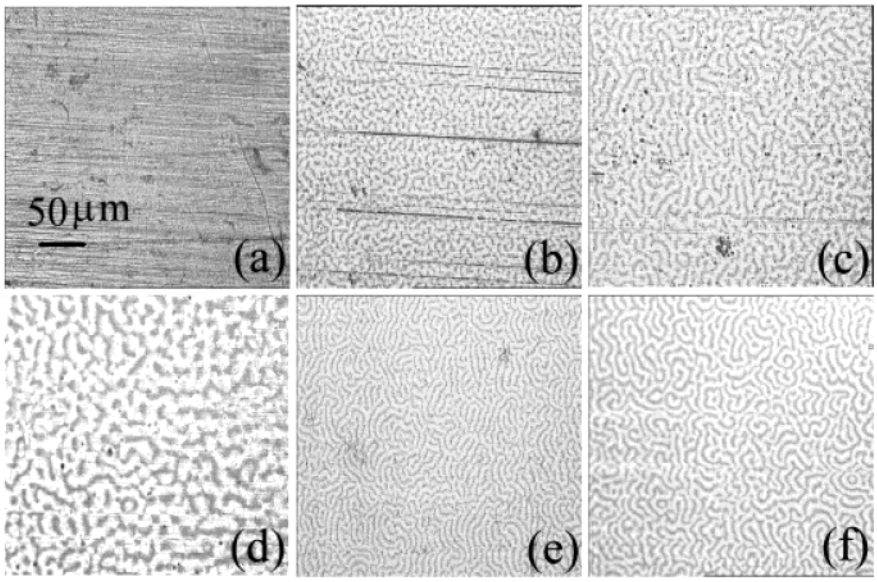

Figure 7. Microscope images for Ag−Sb electrodeposits grown at $t = 120$, 180, 300, 360, 420, and 480 s (from (a) to (f)) from 6.7 g/L APT electrolyte, which shows a change in the stripe spacing as the deposition time proceeds.

An example of plot of the normalized current density vs the deposition time is shown in Figure 4. As can be seen, the experimental data can be well described by eq 10. Thus, the parameter characterizing the kinetics of electrode reactions, $k_i/\sqrt{D_i}$ is determined from the current density−time curves. The obtained result shown in Figure 5 approximately gives

$$\sqrt{\frac{D_2}{D_1}} \approx 5\frac{k_2}{k_1} \tag{11}$$

This relation is similar to eq 1 required for the Turing instability. Unfortunately the experimental values of k_i are unknown. However, since EPMA measurements indicate that the mole fraction of Ag to Sb in the electrolyte is nearly equal to that in the electrodeposits, we may approximately set $k_1 \approx k_2$. In this case, according to eq 11, the diffusion coefficient of Sb becomes larger than that of Ag, which satisfies a condition required from linear stability analysis of the reaction−diffusion systems though this Ag−Sb electrodeposition system is not equivalent to the activator−inhibitor system.

From the current density−time measurements, we can also determine an experimental condition that the stripe patterns emerge. Figure 6 shows a plot of the saturated current density and potential at which stripe patterns are formed or not formed. We find no difference in the morphologies of the Ag−Sb deposits grown at 13 and 16 mA/cm^2. As can be seen, the region where the stripe patterns emerge is very restricted. This suggests that some condition, which may be similar to the Turing instability, will be derived from electrochemical reactions that produce intermediate species.

2. Fourier Transformed Images of the Stripe Patterns. Next, let us examine properties of the time-series stripe patterns of the Ag−Sb electrodeposits. Microscope images from the samples electrodeposited at six different deposition times are shown in Figure 7. Figure 7(a) shows that no stripe pattern is formed, which suggests the presence of some incubation time needed to form the stripe pattern. However, there may be the Sb distribution difference that cannot be found with optical observation. More detailed study using ESCA will be needed to examine the incubation time. Figure 7 is obtained by ex-situ optical observation, but we made several experiments of the transient Ag−Sb film growth in the same way to guarantee the reproducible results. It can be seen that the stripe spacing defined as a distance between the nearest dark stripes in real space changes with the deposition time. But the stripe patterns formed at the different times seem to resemble each other except that the stripe patterns have different stripe spacings. In other words, this implies that the stripe patterns emerge only on different length-scales.

To observe the difference in the deposition rate in the dark and white stripe, we implanted the Ag−Sb electrodeposits grown for 30 min into a polyster resin and polished the cross section of the sample. The difference in the step on the electrodeposit surfaces is not observed by the laser scope microscope (magnification ×2500). However, there may exist the step that cannot be observed with the optical microscopes. More detailed study using AFM will be needed. Figure 7, which shows variation of the stripe spacing with time, indicates that a white (dark) stripe does not always continue to grow on a white (dark) stripe, i.e., electrodeposition proceeds despite the electrodeposit surfaces. Consequently, electrodeposition levels difference in height between the white and dark stripe.

Figure 8 shows the Fourier spectra of the stripe patterns electrodeposited at 300 s and 480 s (corresponding to Figure 7(b) and (e), respectively). It can be seen that one bright but somewhat blur ring appears and one mode of a wavenumber exists. This indicates that the stripe patterns have isotropic and periodic properties in real space, i.e., that there exist the rotational symmetry and one wavenumber characterizing the stripe patterns. If some convection affects the formation of the patterns, some anisotropic pattern such as an array of the dark stripes will appear. In which case, the Fourier spectra of the stripe patterns show bright points or lines. However, the Fourier spectra in this experiment show only one bright ring. Hence, in this study some convection doe not affect the formation of the stripe patterns.

In addition, Fleury et al.[17] and Wang et al.[18] report that electric migration and electroconvection due to the electric field gradient around tip-like electrodeposits affect a morphological transition. In this study, as the Ag−Sb electrodeposits have no tips into the electrolyte at a micron length level, no steep gradient of the electric field takes place. Hence, we can ignore the effects

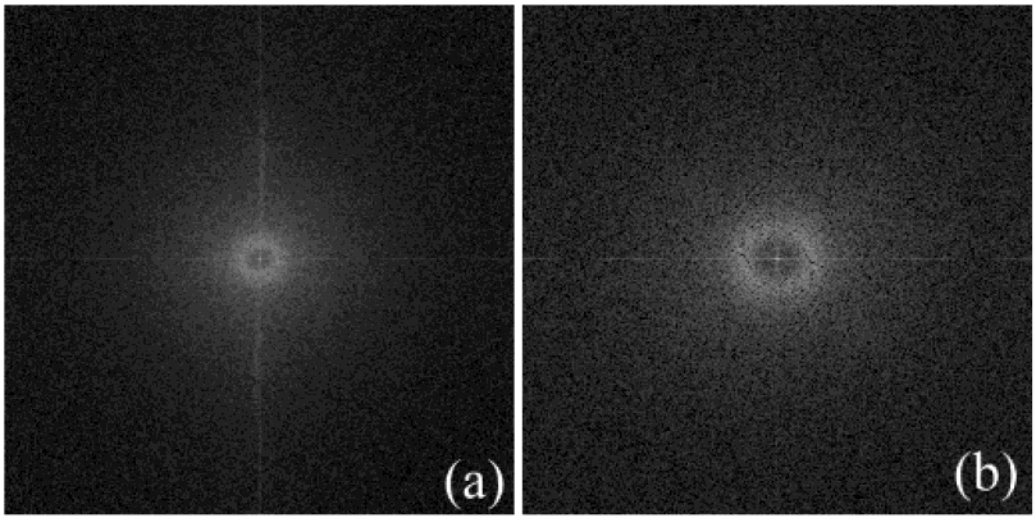

Figure 8. Fourier power spectra of the stripe patterns. These figures (a) and (b) are calculated for the images of Figure 7(b) and (e), respectively. Each spectrum shows the presence of one mode of the wavenumber.

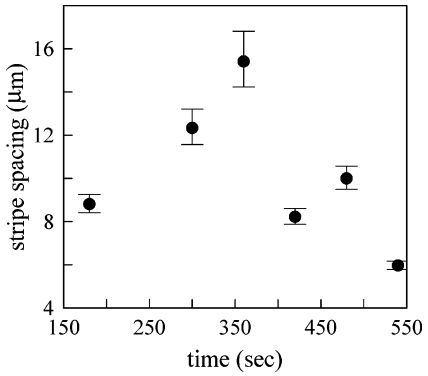

Figure 9. Typical plots of the time dependence of the stripe spacing that is calculated from the Fourier spectra of the stripe patterns.

of electric migration and electroconvection on the formation of the stripe patterns.

In this system, the average current efficiency, which is defined as the ratio of the actual thickness of Ag−Sb deposits to the theoretical expected thickness of Ag−Sb deposits, becomes about 0.92, i.e., 8% of the total current is consumed in producing some gases such as the hydrogen gas. Some convection may occur and produce some anisotropic patterns. However, the Fourier spectra of the stripe patterns obtained in this experiment show that one bright blur ring appears. Hence, in this study convection does not affect the formation of the stripe patterns.

The mode of the wavenumber characterizes the stripe patterns in the Ag−Sb electrodeposits. The stripe spacing can be determined from the wavenumber measured as a distance between the origin and the point in the ring that in Figure 8 has the highest intensity of brightness.

The obtained stripe spacing is plotted in Figure 9 as a function of the deposition time. The stripe spacing shows an oscillatory behavior as opposed to the stable current density−time curves when the stripe patterns are observed. We can measure the area ratio of the dark region to the bright region from binary images of the stripe patterns. The dark and bright regions are determined by the number of pixels in the binary image transformed from the microscope image.

Figure 10 shows a plot of the area ratio of the dark region to the total area vs the deposition time. It is obvious that the ratio is independent of the deposition time, which result well explains that the current density−time curves are stable when the stripe patterns are observed. The stripe spacing changes in the growth time with the area ratio of the dark region to the bright region fixed. In addition, in this case, it is found that the average stripe spacing remains in a range of about 6 to 17 μm. This implies

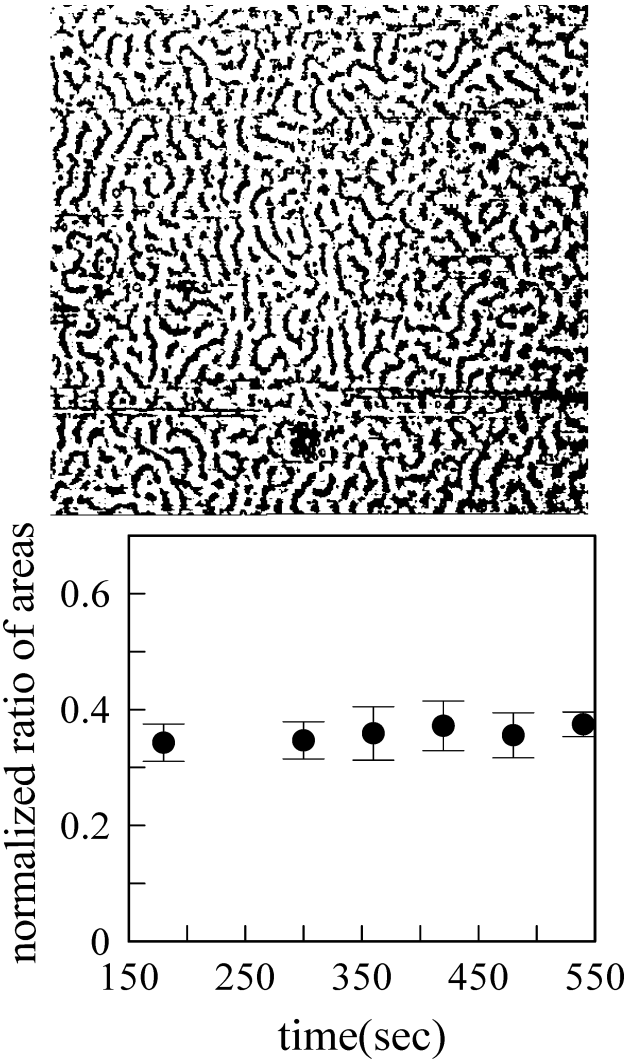

Figure 10. Typical plots of the ratio of the dark region to the total area vs the deposition time. The ratio of the dark region to the total area is calculated from the number of pixels in the binary images.

that the minimum wavenumber may be related to the critical wavenumber derived in the reaction−diffusion systems.[5]

These experimental results are obtained by ex-situ optical observation. To analyze the transient behavior of the stripe pattern in detail, we need experimental results by in-situ optical observation, which remains to be done.

Conclusions

We have investigated transient changes in stripe patterns of Ag−Sb thin films electrodeposited from the aqueous electrolyte. The measurements of the current density for the impulse potential applied during electrodeposition reveal that the stripe patterns are formed within the limited ranges of potential and current density. In addition, the current density−time curves, which show no oscillatory behavior when the stripe patterns are formed, are in good agreement with the solutions of electrode reaction equations. The ratios of the kinetic constant to diffusion coefficient obtained from the current density−time curves are discussed in view of the necessary condition for the Turing instability in reaction−diffusion systems. Fourier analysis of the time-series stripe images shows that the stripe spacing changes with the area ratio of the bright region to the dark region fixed. The presence of the minimum wavenumber is shown, which may be related to the critical wavenumber derived in the reaction−diffusion systems.

Acknowledgment. M.S. thanks Mr. Hideki Higa in the University of the Ryukyus for the experimental preparations.

References and Notes

(1) Cross, M. C.; Hohenberg, P. C. *Rev. Mod. Phys.* **1993**, *65*, 851.
(2) Koch, A. J.; Meinhardt, H. *Rev. Mod. Phys.* **1994**, *66*, 1481.
(3) DeKepper, P.; Epstein, I. R.; Kustin, K.; Orbán, *J. Phys. Chem.* **1982**, *86*, 170.
(4) Kadar, S.; Lengyel, I.; Epsrein, I. R. *J. Phys. Chem.* **1995**, *99*, 4504.
(5) Kapral, K.; Showalter, K. *Chemical Waves and Patterns*; Kluwer Academic Press: Dordrecht, 1995; pp 367−369.
(6) Witten, T. A.; Sander, L. M. *Phys. Rev. Lett.* **1981**, *19*, 1400.
(7) Barabási, A.-L.; Stanley, H. E. *Fractal Concepts in Surface Growth*; Cambridge Press: Cambridge, 1995.
(8) Raub, E.; Schall, A. *Z. Metallk* **1938**, *30*, 149.
(9) Kristev, I.; Nikolova, M.; Nakada, I. *Electrochim. Acta* **1989**, *8*, 1219.
(10) Krastev, I.; Kopper, M. T. M. *Physica A* **1995**, *213*, 199.
(11) Delahay, P.; Stiehl, G. *J. Chem. Phys.* **1952**, *74*, 3500.
(12) Rubin, H.; Collins, F. C. *J. Phys. Chem.* **1954**, *58*, 958.
(13) Yang, L.; Dolnik, M.; Zhabotinsky, M.; Epstein, I. R. *J. Chem. Phy.* **2002**, *117*, 7259.
(14) Leimkühler, G.; Kerkamm, I.; R-Koch, R. *J. Electrochem. Soc.* **2002**, *149*, C474.
(15) Krasrev, I.; Zielonka, A.; Nakabayashi, S.; Inokuma, K. *J. Appl. Electrochem.* **2001**, *31*, 1041.
(16) Crank, J. *The Mathematics of Diffusion*; Oxford Press: London, 1975.
(17) Fleury, V.; Kaufman, J. H.; Hibbert, D. B. *Nature* **1994**, *367*, 435.
(18) Wang, M.; V-Enckevort, W. J. P.; Ming, N-b; Bennema, P. *Nature* **1994**, *367*, 438.